Supplementary Information for

Amplification Label of core-shell CdSe@CdS QDs Sensitized GO for Signal-on Photoelectrochemical Immunosensor of Amyloid β-protein

Jinhui Feng, Faying Li, Xiaojian Li, Xiang Ren, Dawei Fan, Dan Wu, Hongmin Ma, Bin Du*, Nuo Zhang*, Qin Wei

Key Laboratory of Interfacial Reaction & Sensing Analysis in Universities of Shandong, School of Chemistry and Chemical Engineering, University of Jinan, Jinan 250022, PR China

* Corresponding author

E-mail: dubin61@gmail.com

zhangnuoujn@163.com

Fax: +86-531-82765969;

Tel: +86-531-82767872

2.1 Materials and Apparatus

Materials: The urea and $FeSO_4 \cdot 7H_2O$ were purchased from Sinopharm Chemical Reagent Co. Ltd. (Beijing, China). $HAuCl_4 \cdot 4H_2O$ were obtained from Sigma-Aldrichco., Ltd. (Beijing, China). $CdCI_2 \cdot 2.5H_2O$, $Na_2S \cdot 9H_2O$, SeO_2, and $NaBH_4$ were purchased from Sinopharm Chemical Reagent Co. Ltd. (Beijing, China). 1-ethyl-3-(3-dimethylaminopropyl) carbodiimide hydrochloride (EDC, 98.5%) and N-hydroxysuccinimide (NHS) were obtained from Aladdin Chemistry Co. Ltd. (Shanghai, China). Bovine serum albumin (BSA, 96-99%) was purchased from Sigma reagent Co., Ltd. (St. Louis, MO, USA). The indium tin oxide (ITO) glass was obtained from Zhuhai Kaivo Electronic Components Co., Ltd. China. All other chemicals were of analytical grade and were directly used without further purification. The ultrapure water with a specific resistivity (≥18.2 MΩ) obtained from a Millipore water purification system was used in all solutions.

Apparatus: Scanning electron microscope (SEM) images and energy dispersive spectrometry (EDS) were obtained using a field emission SEM (Zeiss, Germany). The transmission electron microscopy (TEM) and HRTEM images were obtained using a JEOL JEM-2100F TEM (Japan). X-ray diffraction (XRD) patterns were performed with D8 advance X-ray diffractometer (Bruker AXS, Germanyz). Fourier transform infrared spectroscopy (FT-IR) spectra was carried out on Bruker VERTEX 70 spectrometer. X-ray photoelectron spectroscopy (XPS) analysis was performed on ESCALAB 250 X-ray photoelectron spectrometer with an Al Kα radiation source (1486.6 eV). Electrochemical impedance spectroscopy (EIS) analysis was performed with an

RST5200F electrochemical workstation (Zhengzhou Shiruisi Technology Co., Ltd, China).

Synthesis of Mercaptopropanoic Acid (MPA)-capped core-shell CdSe@CdS QDs. In details, 2×10^{-3} mol of $CdCl_2\cdot2.5H_2O$ as the cadmium source was dissolved in 50 mL ultrapure water, then 0.3 mL MPA was added under stirring and maintained for 30 min. The pH of the solution was adjusted to 10.58 by addition of 1 mol L^{-1} NaOH solution. The 3×10^{-4} mol of SeO_2 and 1×10^{-3} mol of $NaBH_4$ were added into above mixed solution under stirring for 1 h. Then, 4×10^{-4} mol of $Na_2S\cdot9H_2O$ in 5 mL ultrapure water was added into above solution under stirring for 30 min. Subsequently, the solution was transferred into 100 mL Teflon-lined stainless steel autoclave. After maintaining at 110 ℃ for 9 h, the cooled sample was washed with ultrapure water.

Synthesis of GO/CdSe@CdS QDs. Specifically, 30 mg of GO dispersed in ultrapure water and ultrasonicated for 24 h. After centrifuged at 3000 rpm for 10 min, the supernatant was collected for further using. 10 mg of CdSe@CdS QDs was dispersed in the collected GO supernatant and ultrasonicated for 6 h to obtain the GO/CdSe@CdS QDs.

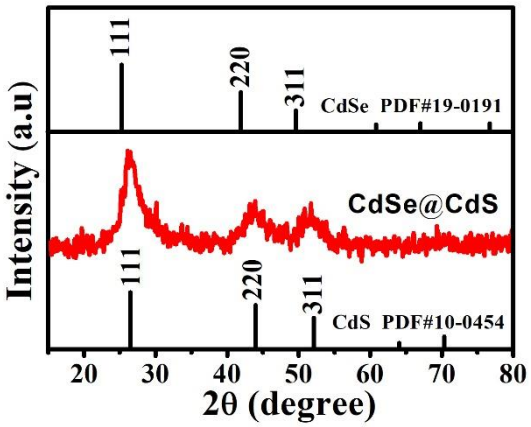

Figure S1. The XRD patterns of CdSe@CdS core@shell QDs

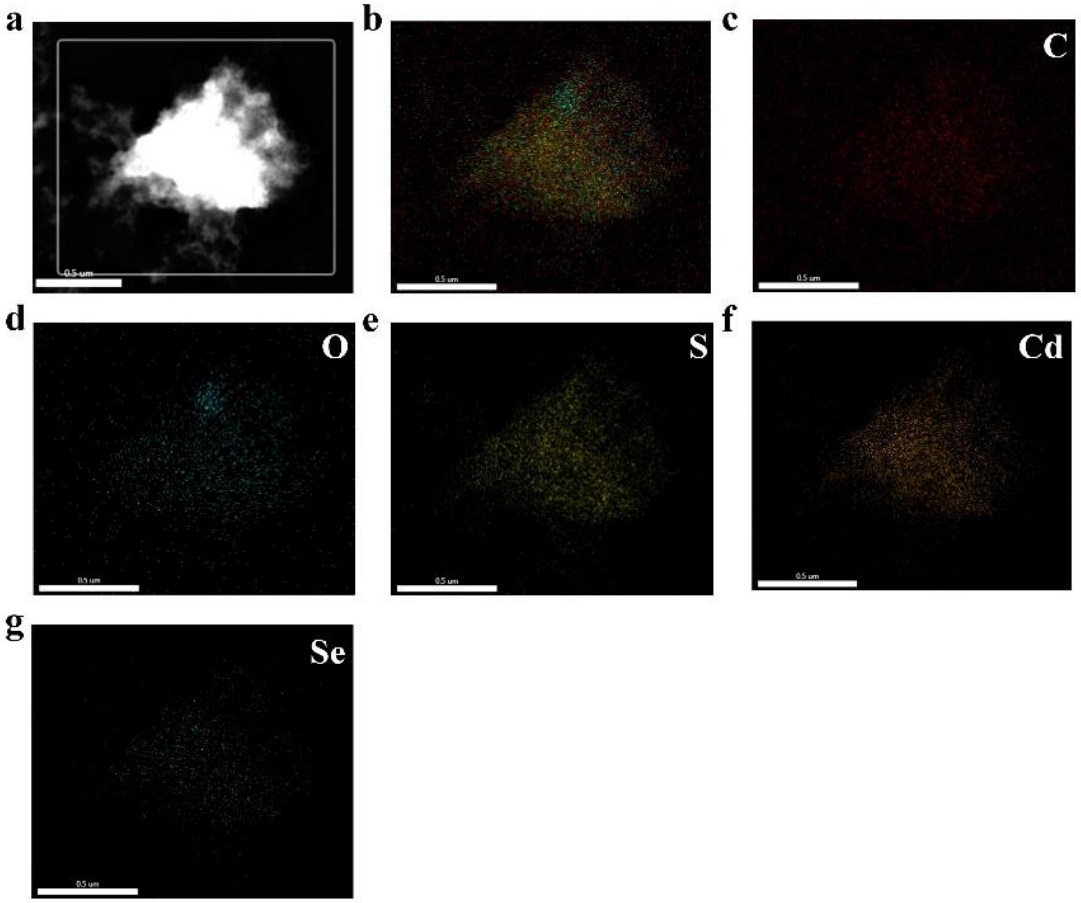

Figure S2 (a) high-angle annular dark-field scanning TEM; corresponding Energy-dispersive X-ray mapping: (b) merged imagine, (c) C, (d) O, (e) S, (f) Cd and (g) Se

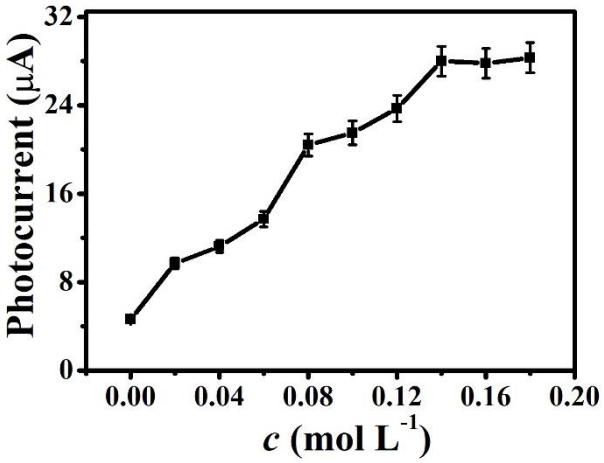

Figure S3. Photocurrent responses of the PEC biosensor at different concentration of AA (0.1 ng mL^{-1} Aβ, error bars=SD (n=5)).

As exhibited in Figure S3, the photocurrent intensity was much enhanced with AA concentration from 0.00 to 0.14 mol L^{-1} and then reached to level off due to the saturation of electron donor. Thus, the optimal concentration of AA was chosen as 0.14 mol L^{-1}.

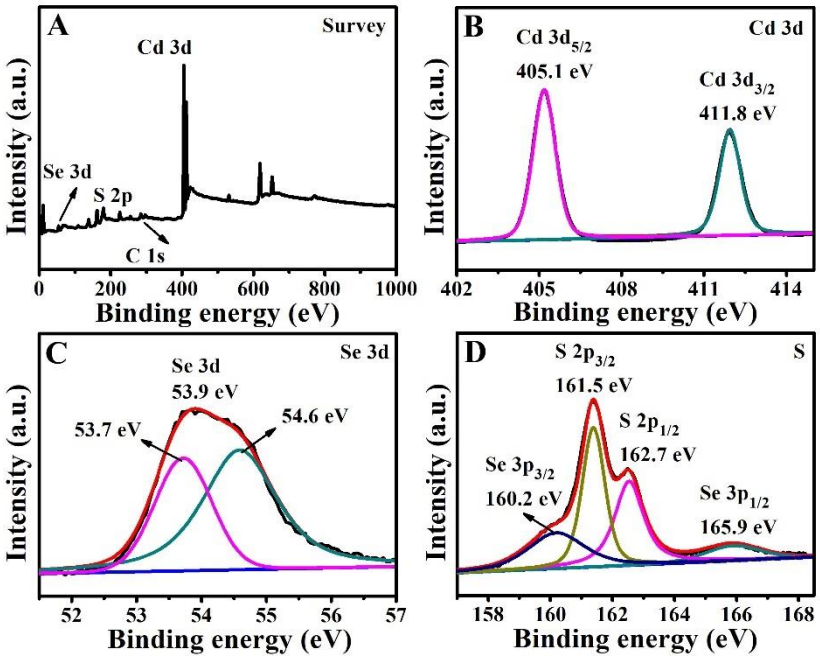

Figure S4. XPS survey spectrum of CdSe@CdS QDs composite: (A) survey spectrum; (B) Cd 3d; (C) Se 3d; (D) S 2p.

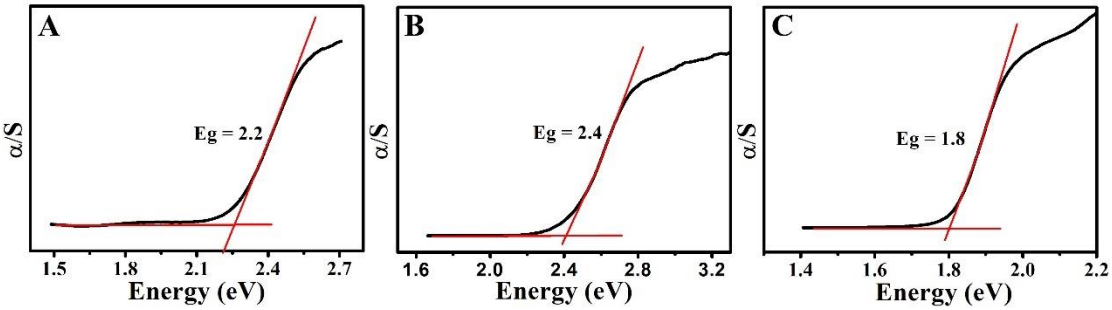

Figure S5 UV−vis diffuse reflectance spectroscopy of (A) α-Fe_2O_3, (B) CdS and (C) CdSe

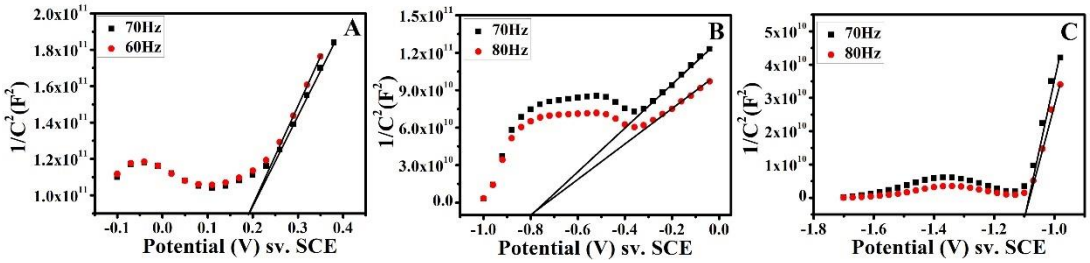

Figure S6 (A)-(C) Mott-Schottky curves of α-Fe_2O_3, CdS and CdSe in a 0.2 mol/L Na_2SO_4 aqueous solution

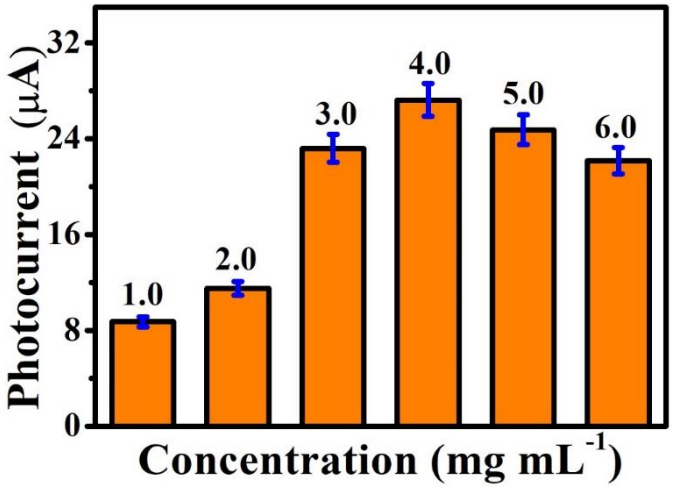

Figure S7 Photocurrent responses of the PEC biosensor at different concentration of Au NPs/α-Fe_2O_3 at 0 V (orange columns, 0.1 ng mL^{-1} Aβ, error bars=SD (n=5)).

The photocurrent response of this developed biosensor was influenced by the concentration of Au NPs/α-Fe_2O_3. The effect of the concentration of Au NPs/α-Fe_2O_3 on the photocurrent responses was examined at the ranges from 1.0 to 6.0 mg mL^{-1}. As shown in Figure. S7, it was found that the photocurrent value was maximum when the concentration at 4.0 mg mL^{-1}. Therefore, the concentration of 4.0 mg mL^{-1} was adopted as the optimal concentration of Au NPs/α-Fe_2O_3 in this work.

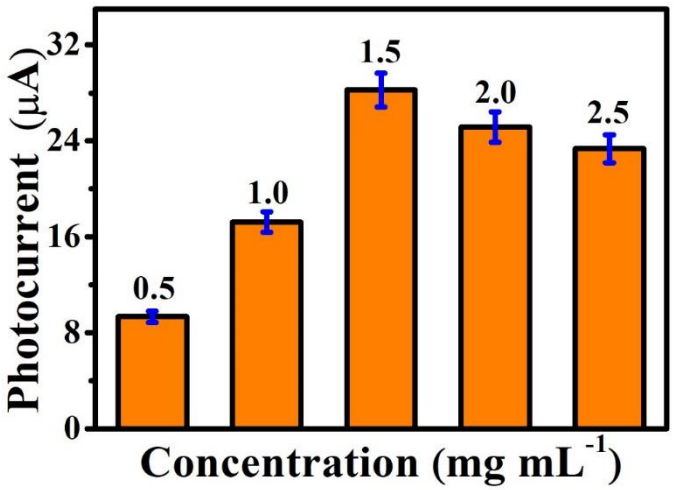

Figure S8 Photocurrent responses of the PEC biosensor at different concentration of GO/CdSe@CdS QDs at 0 V (orange columns, 0.1 ng mL^{-1} Aβ, error bars=SD (n=5)).

As the signal application label, the concentration of GO/CdSe@CdS QDs has an important influence on the photocurrent responses. Figure. S8 showed the photocurrent responses increased as the concentration ranged from 0.5 to 1.5 mg mL^{-1}, then presented a decreased in photocurrent between the concentrations from 1.5 to 2.5 mg mL^{-1}. Therefore, 1.5 mg mL^{-1} was chosen as the optimal concentration of GO/CdSe@CdS QDs.

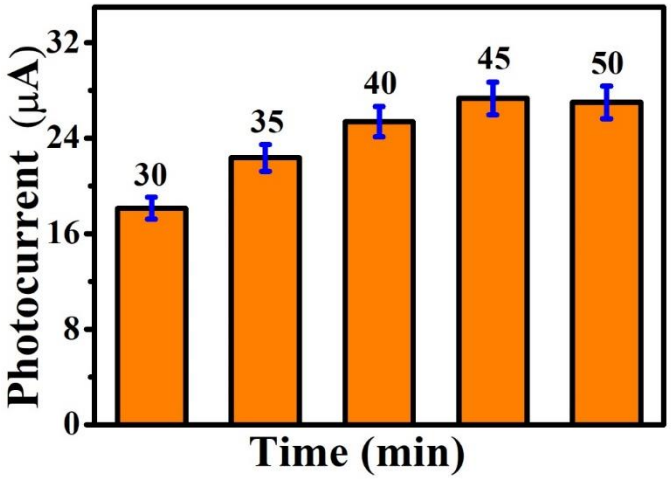

Figure S9 Photocurrent responses of the PEC biosensor at different incubation time of Ab_1- Aβ at 0 V (orange columns, 0.1 ng mL^{-1} Aβ, error bars=SD (n=5)).

The photocurrent response of this developed biosensor was also influenced by the incubation time of Ab_1-Aβ. As demonstrated in Figure S9, the photocurrent response for detecting Aβ was enhanced with the increasing times then tended to be constant after 45 min. Therefore, 45 min was selected as the Ab_1-antigen incubation time.

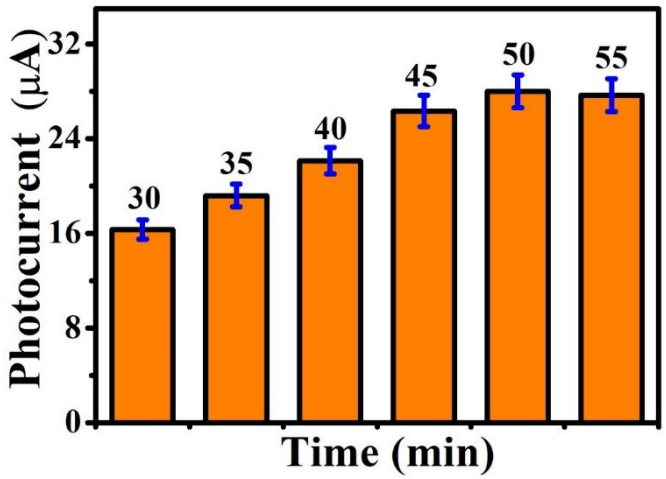

Figure S10 Photocurrent responses of the PEC biosensor at different incubation time of Aβ-Ab_2 at 0 V (orange columns, 0.1 ng mL^{-1} Aβ, error bars=SD (n=5)).

Besides, the influence of incubation time for the Aβ-Ab_2 label reaction was investigated in Figure S10. Obviously, with exceeding the incubation time, the response value quickly elevated from 30 to 50 min, and then leveled off. Considering the determination efficiency, 50 min was chosen for the antigen-Ab_2 label reaction in the further studies.

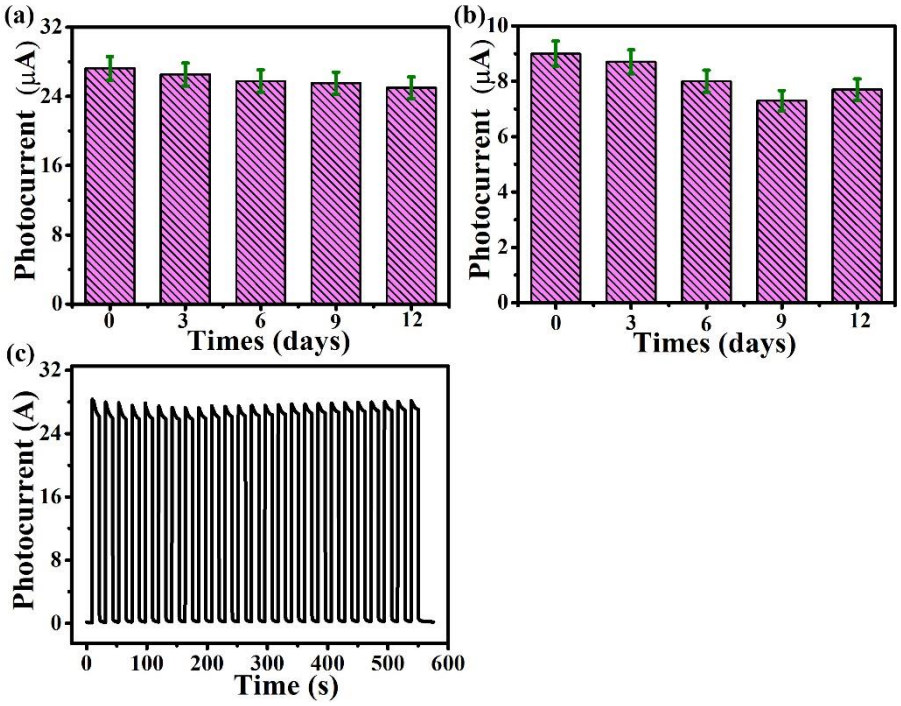

Figure. S11 (a) $c_{A\beta}$ = 0.1 ng mL^{-1} and (b) $c_{A\beta}$ = 0 ng mL^{-1} the storage stability study of the Aβ immunosensor, respectively, (c) photocurrent stability evaluation of the PEC immunosensor under several on/off irradiation cycles for 600 s, $c_{A\beta}$ = 0.1 ng mL^{-1}

Table S1 Simulation parameters of the equivalent circuit components

Electrode	R_s (Ω)	R_{et} (Ω)	C_{dl} (F)	Z_W
ITO	68.60	14.38	2.614×10^{-6}	0.00884
ITO/α-Fe_2O_3/Au NPs	68.12	9.455	2.499×10^{-6}	0.00936
ITO/α-Fe_2O_3/Au NPs/Ab_1	68.05	21.45	3.490×10^{-6}	0.00939
ITO/α-Fe_2O_3/Au NPs/Ab_1/BSA	70.09	30.63	3.532×10^{-6}	0.00817
ITO/α-Fe_2O_3/Au NPs/Ab_1/BSA/Aβ	70.95	53.28	4.593×10^{-6}	0.00808
ITO/α-Fe_2O_3/Au NPs/Ab_1/BSA/Aβ/GO/CdSe@CdS QDs-Ab_2	70.29	71.16	4.109×10^{-6}	0.00786

Table S2 Comparison of different methods for the detection of Aβ

Method	Signal label	Target	Detection limit	Reference
Electrochemiluminescent	GOD@Ce:ZONFs-Lum	Aβ	0.052 pg ml^{-1}	[1]
Electrochemiluminescent	Ru@FGA-Pd	PSA	0.056 pg ml^{-1}	[2]
Electrochemistry	Ag NCs	AFP	0.8 pg ml^{-1}	[3]
PEC	AgNCs-GR	CEA	1.0 pg ml^{-1}	[4]
PEC	CdTe−GOx	AFP	0.13 pg ml^{-1}	[5]
PEC	GO/CdSe@CdS QDs	Aβ	0.02 pg ml^{-1}	This method

Table S3. Five sample analysis used the designed method and the ELISA

Sample	1	2	3	4	5
This method (ng mL^{-1}) [α]	0.119	0.103	0.147	0.049	0.062
ELISA (ng mL^{-1}) [α]	0.118	0.104	0.149	0.048	0.063
Relative deviation (%)	0.85	-0.96	-1.34	2.08	-1.58

[α] Average value from five detections.

Table S4. Analytical Application of the Sensor in a Real Sample

Aβ in artificial cerebrospinal (ng/mL)	Added amounts (ng/mL)	The detection content (ng/mL)	Average value (ng/mL)	RSD (%,n=5)	Recovery (%,n=5)
Sample 1	0.01	0.125, 0.132, 0.124 0.132, 0.135	0.129	3.72	99.67
	0.10	0.223, 0.220, 0.212 0.232, 0.215	0.221	3.52	100.4
	1.0	1.120, 1.127, 1.137 1.200, 1.120	1.141	2.96	101.8
	10	10.02, 10.12, 10.31 10.16, 10.23	10.17	1.08	100.5

1. J. Wang, Y. Zhuo, Y. Zhou, H. Wang, R. Yuan and Y. Chai, *ACS Appl. Mater. Interfaces*, 2016, **8**, 12968-12975.
2. L. Yang, Y. Li, Y. Zhang, D. Fan, X. Pang, Q. Wei and B. Du, *ACS Appl. Mater. Interfaces*, 2017, **9**, 35260-35267.
3. B. Zhang, B. Liu, J. Zhou, J. Tang and D. Tang, *ACS Appl. Mater. Interfaces*, 2013, **5**, 4479-4485.
4. J. Song, J. Wang, X. Wang, W. Zhao, Y. Zhao, S. Wu, Z. Gao, J. Yuan and C. Meng, *Biosens Bioelectron*, 2016, **80**, 614-620.
5. L. YJ, M. MJ and Z. JJ, *Anal. Chem.*, 2012, **84**, 10492-10499.